Crystal and Molecular Structure of β-Maltose Octaacetate. A Model in Retrospect for Amylose Triacetate?

F. Brisse,* R. H. Marchessault,*‖ S. Pérez,† and P. Zugenmaier‡

Contribution from the Département de Chimie, Université de Montréal, Montreal, H3C 3V1, Canada, the Centre de Recherches sur les Macromolécules Végétales, 53X, 38041 Grenoble Cédex, France, and the Institut für Physikalische Chemie der Technischen Universität Clausthal, D-3392 Clausthal-Zellerfeld, Federal Republic of Germany.
Received April 21, 1982

Abstract: The crystal structure of β-maltose octaacetate, $C_{28}H_{38}O_{19}$, has been established by direct methods from 3391 independent reflections and refined by a least-squares block-diagonal approximation to a final R value of 0.061. The crystals belong to the orthorhombic system, space group $P2_12_12_1$, and have a unit cell of dimensions a = 5.733 (1), b = 23.771 (6), and c = 25.632 (6) Å. The two D-glucose residues have the $^4C_1$ pyranose conformation and are α(1→4) linked. The conformational angles Φ and Ψ at the glycosidic linkage have the values of −29 and −36°, respectively. The acetate substituent at C(6) of the reducing residue is in the *gg* conformation, but in the nonreducing residue there is a disorder of the C(6) acetate group. Two distinct orientations are observed in equal proportions, one having the *gt* conformation and the other having the *tg* conformation. A conformational analysis using the β-maltose acetate geometry reveals that the energy map computed as a function of the rotations about Φ and Ψ angles is not significantly influenced by the presence of the C(6) acetates. A survey of the distribution of the Φ angles in all known α-linked D-glucose residues discloses a binodal distribution; each node corresponds to the occurrence or the nonoccurrence of hydrogen bonding between contiguous residues. A molecular modeling of the behavior of β-maltose octaacetate in solution is proposed and tested against the experimental H(1)–H(4′) distances derived from T_1 NMR experiments.

Introduction

The modern approach for the analysis of polysaccharide crystal structures necessarily involves high-speed computers and specialized programs for modelling the relation between diffracted intensities and stereochemistry.[1,2] The critical paper oligosaccharide this approach, by Sarko and Marchessault[1] (1967), involved a fiber diagram of amylose triacetate whose crystalline form was first observed by Whistler and Schieltz.[3] This fiber diagram shows clearly the characteristics of the helix transform which eventually was resolved into a 14/3 helix. Not counting hydrogens, the unit cell encompasses 560 atoms whose positions in space had to be resolved from 21 pieces of observed information. This total underdetermination was handled by a trial-and-error approach based on certain key assumptions which are well known in present procedures for studying polysaccharides.[4-6]

One of the important assumptions involved the idea that resonance in the acetate ester link was sufficiently strong to fix the acetate groups in a trans-planar conformation. Subsequent studies on oligosaccharide acetates and acetylated carbohydrate acetates have shown the validity of this assumption.[7,8] At the time the amylose acetate analysis was made, crystallographic analyses on related single crystals of oligosaccharide acetates were not available. The present study on maltose octaacetate, some 15 years later, provides an opportunity to compare the acetate positions derived for the polysaccharide with those which are found in the disaccharide model compound. Similar studies on cellobiose octaacetate[9] and cellotriose undecaacetate[10] were invaluable for refining the structures of cellulose triacetate I[11] and II.[12] *O*-Acetylpyranose derivatives of carbohydrates and oligosaccharides usually crystallize more easily than the naturally occurring carbohydrate. For this reason, a number of acetate derivatives of mono-, di-, and trisaccharides have been reported. A recent publication analyzes the conformation of these molecules and uses semiempirical potential energy calculations in order to rationalize the observed conformations.[13] The survey clearly establishes that the conformation of the acetyl group in carbohydrate acetates is planar trans, the plane being approximately perpendicular to the mean plane of the pyranose ring in the case of secondary hydroxyls. Primary hydroxyl acetates are also planar trans but show a preference for either the *gt* or *gg* conformation with respect to the pyranose ring.[14] The two different rotamers are often found in different residues in a single oligosaccharide acetate.[15]

The influence of the acetate substituent on the ring geometry is minor as may be deduced by comparing *O*-acetyl-β-D-cellobiose and β-cellobiose.[7] On the other hand, the introduction of acetate substituents in the disaccharide removes the possibility of an

Table I. Crystal Data for β-Maltose Octaacetate

$C_{28}H_{38}O_{19}$	MW = 678.6	F(000) = 1432 e
a = 5.733(1), b = 23.771(6), c = 25.632(6) Å		
V = 3493.0 Å^3, orthorhombic, $P2_12_12_1$		
d_o = 1.29, d_c = 1.290, Mg m^{-3}, Z = 4		
μ(CuKα) = 0.91 mm^{-1}		λ(CuKᾱ) = 1.54178 Å

(1) A. Sarko and R. H. Marchessault, *Science*, **154**, 3757 (1966).
(2) A. Sarko and R. H. Marchessault, *J. Am. Chem. Soc.*, **89**, 6454 (1967).
(3) R. L. Whistler and N. C. Schieltz, *J. Am. Chem. Soc.*, **65**, 1436 (1943).
(4) R. H. Marchessault and A. Sarko, *Adv. Carbohyd. Chem.*, **22**, 421 (1967).
(5) S. Arnott and S. E. *Scott*, *J. Chem. Soc., Perkin Trans. 2*, 324 (1972).
(6) G. A. Jeffrey and A. D. French, "Molecular Structure by Diffraction Methods", ACS Symposium Series, No. 141, A. D. French and K. C. H. Gardner, Eds., American Chemical Society, Washington, D.C., 1980.
(7) R. H. Marchessault and P. R. Sundararajan, *Pure Appl. Chem.*, **42**, 399 (1975).
(8) R. H. Marchessault and H. Chanzy, "Cellulose Chemistry and Technology", ACS Symposium Series, No. 48, American Chemical Society, Washington, D.C., 1977, p 3.
(9) F. Leung, H. Chanzy, S. Pérez, and R. H. Marchessault, *Can. J. Chem.*, **54**, 1365 (1976).
(10) S. Pérez and F. Brisse, *Acta Crystallogr., Sect. B*, **33**, 2578 (1977).
(11) A. J. Stipanovic and A. Sarko, *Polymer*, **19**, 3 (1978).
(12) E. Roche, H. Chanzy, M. Boudeulle, R. H. Marchessault, and P. R. Sundararajan, *Macromolecules*, **11**, 86 (1978).
(13) S. Pérez, J. St.-Pierre, and R. H. Marchessault, *Can. J. Chem.*, **56**, 2866 (1978).
(14) M. Sundaralingam, *Biopolymers*, **6**, 189 (1968).
(15) S. Pérez and F. Brisse, *Biopolymers*, **17**, 2083 (1978).

* Author to whom correspondence should be addressed at Université de Montréal.
‖ Author to whom correspondence should be addressed at the Xerox Research Centre of Canada, Mississango, Ontario, L5L 1J9.
† Centre de Recherches sur les Macromolécules Végétales.
‡ Technischen Universität Clausthal.

0002-7863/82/1504-7470$01.25/0

Table II. Atomic Positional Parameters and Their Esd's in Parentheses ($\times 10^4$)

BETA MALTOSE OCTAACETATE

ATOM	X	Y	Z
O(1)	-1813(7)	-6622(1)	-2148(1)
O(2)	-1707(8)	-7743(2)	-1921(1)
O(3)	-1640(8)	-8157(2)	-2948(2)
O(4)	-1794(8)	-7262(2)	-3695(1)
O(5)	-5304(8)	-6710(2)	-2620(1)
O(61)	-5201(22)	-6383(4)	-3973(4)
O(62)	-6355(23)	-6018(4)	-3627(4)
OA(2)	-4627(9)	-8112(2)	-1475(2)
OA(3)	2199(9)	-8076(2)	-2944(3)
OA(4)	-4132(12)	-7784(2)	-4200(2)
OA(61)	-3782(28)	-5938(6)	-4695(4)
OA(62)	-7904(29)	-6170(5)	-4405(4)
C(1)	-3926(11)	-6919(2)	-2209(2)
C(2)	-3271(11)	-7528(2)	-2316(2)
C(3)	-1966(10)	-7573(2)	-2820(2)
C(4)	-3354(12)	-7312(2)	-3260(2)
C(5)	-4211(12)	-6717(3)	-3121(2)
C(6)	-6036(16)	-6529(3)	-3499(3)
CA(2)	-2566(13)	-8060(3)	-1540(2)
CA(3)	534(12)	-8351(3)	-3006(3)
CA(4)	-2335(15)	-7529(3)	-4141(3)
CA(61)	-4726(42)	-5962(7)	-4180(7)
CA(62)	-7380(39)	-5847(6)	-4094(5)
CM(2)	-663(14)	-8330(3)	-1232(3)
CM(3)	462(17)	-8953(3)	-3146(4)
CM(4)	-449(19)	-7478(5)	-4521(3)
CM(61)	-3871(54)	-5628(9)	-3833(8)
CM(62)	-7439(67)	-5231(9)	-4139(8)
O(1')	1590(8)	-4940(2)	-929(2)
O(2')	-254(9)	-5886(2)	-439(1)
O(3')	-3703(7)	-6469(1)	-1068(1)
O(5')	563(7)	-5290(1)	-1725(1)
O(6')	-2245(9)	-5245(2)	-2618(2)
OA(1')	5053(8)	-4869(2)	-1336(2)
OA(2')	-3514(13)	-5501(3)	-113(2)
OA(3')	-1778(8)	-7130(2)	-606(2)
OA(6')	-742(17)	-4682(3)	-3204(3)
C(1')	1140(11)	-5443(2)	-1211(2)
C(2')	-901(11)	-5726(2)	-959(2)
C(3')	-1531(11)	-6245(2)	-1265(2)
C(4')	-1874(11)	-6114(2)	-1844(2)
C(5')	174(11)	-5771(2)	-2049(2)
C(6')	-187(15)	-5551(3)	-2596(2)
CA(1')	3717(13)	-4700(2)	-1032(3)
CA(2')	-1759(17)	-5744(3)	-49(3)
CA(3')	-3565(11)	-6912(2)	-721(2)
CA(6')	-2410(18)	-4809(4)	-2944(3)
CM(1')	4061(19)	-4190(4)	-695(4)
CM(2')	-742(23)	-5937(4)	452(3)
CM(3')	-5925(13)	-7053(3)	-525(3)
CM(6')	-4627(19)	-4518(4)	-2900(5)

intramolecular hydrogen bond in the acetylated disaccharide, and it was expected that this would perturb the Φ–Ψ dihedral angle pair which determines the orientation of the two pyranose rings with respect to each other. However, a comparison of the natural and acetylated disaccharide shows that angle Φ is much less disturbed than angle Ψ. This has been interpreted as a manifestation of the exo-anomeric effect.[16] One of the purposes of this study was also to compare the Φ–Ψ pair for maltose with the equivalent pair in maltose octaacetate in order to see if this same manifestation of the exo-anomeric effect would be found, since intramolecular H-bonding between O(2)···O(3) is an integral part of the several maltose studies reported.[17-19]

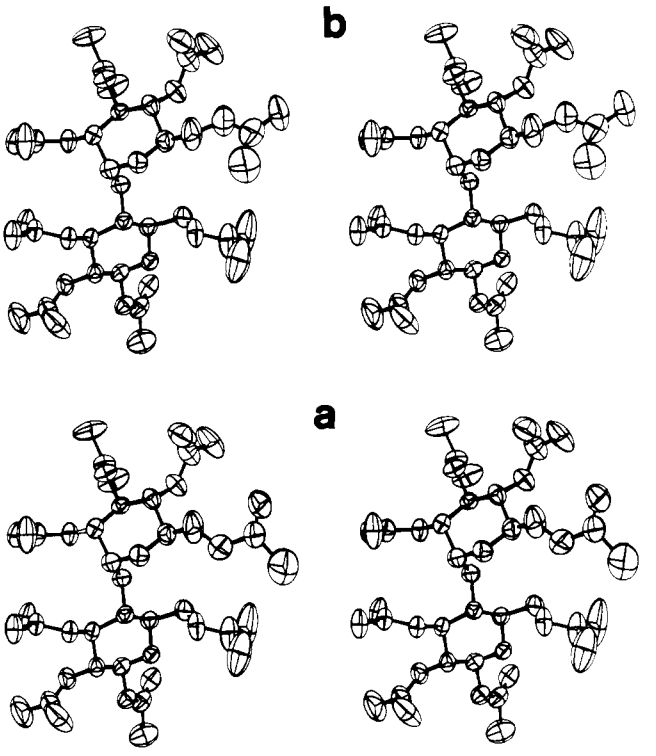

Figure 1. Stereoscopic view of β-maltose octaacetate molecules. (a) *gt* conformation at C(6) and (b) *tg* conformation at C(6).

Experimental Section

Crystals of 1,2,3,6-tetra-*O*-acetyl-4-*O*-(2,3,4,6-tetra-*O*-acetyl-α-D-glucopyranosyl)-β-D-glucopyranose were slowly grown from an ethanolic solution. Precession photographs indicated an orthorhombic unit cell. The space group $P2_12_12_1$ was chosen although there were some very weak 00*l* reflections (*l*, odd) on the diffraction films. This point will be discussed later. Crystal data of interest are summarized in Table I. A crystal with dimensions 0.30 × 0.36 × 0.44 mm was used for data collection on a Nonius CAD4 diffractometer. The intensities were collected in the ω–2θ scan mode using graphite monochromatized Cu Kα with a scan range of $\Delta\omega = (0.75 + 0.35 \tan\theta)°$. Data were collected up to $2\theta = 140°$ for a total 3789 reflections of which 2933 were nonzero. Lorentz and polarization corrections were applied, but no absorption correction was made. The structure was solved using the multisolution program MULTAN.[20] All the nonhydrogen atoms except those of the two C(6) acetates were located on the first *E* map. Most of the remaining nonhydrogen atoms were found on the ΔF synthesis. The structure was refined by the block-diagonal least-squares method where the function minimized was $\Sigma w(\Delta F)^2$ with *w* based on the counting statistics. In the vicinity of the C(6) acetate a Fourier difference map indicated the existence, in equal proportions, of two distinct orientations of the acetate group (*gt* and *tg* conformations). Both were included in the refinement, each with a 0.5 occupancy. The final atomic coordinates are listed in Table II. The final *R* value was 0.079 for all measured reflections and 0.061 for nonzero reflections.

A final ΔF synthesis showed some relatively small fluctuations in residual electron density, from −0.18 to 0.28 e Å^{-3}, in the vicinity of the C(6) acetate group indicating that there still was a slight disorder in this region. The existence of two distinct orientations for the C(6) acetate could explain the existence of the weak 00*l* (*l*, odd) reflections. The ordering of the β-maltose octaacetate molecules with alternating *gt* and *tg* conformations in the *c* direction would destroy the 2_1 symmetry. Therefore, the 00*l* (*l*, odd) reflections would be observed but only weakly since only the acetates (4 atoms out of a total of 47) would not be symmetry related. The atomic scattering factors were taken from ref[21] for O and C atoms and from ref[22] for H atoms. The anisotropic thermal parameters for O and C atoms are listed in Table III. The hydrogen

(16) S. Pérez and R. H. Marchessault, *Carbohyd. Res.*, **65**, 114 (1978).
(17) G. J. Quigley, A. Sarko, and R. H. Marchessault, *J. Am. Chem. Soc.*, **92**, 5834 (1970).
(18) M. E. Gress and J. A. Jeffrey, *Acta Crystallogr., Sect. B*, **33**, 2490 (1977).
(19) S. S. C. Chu and J. A. Jeffrey, *Acta Crystallogr., Sect. B*, **23**, 1038 (1967).
(20) G. Germain, P. Main, and M. M. Woolfson, *Acta Crystallogr., Sect A*, **27**, 368 (1971).
(21) D. T. Cromer and J. T. Waber, *Acta Crystallogr.*, **18**, 104 (1965).
(22) R. F. Stewart, E. R. Davidson, and W. T. Simpson, *J. Chem. Phys.*, **42**, 3175 (1965).

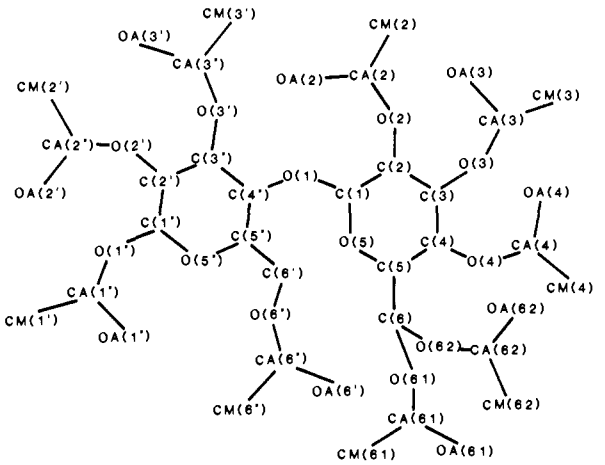

Figure 2. Numbering of the atoms, bond distances, and angles in β-maltose octaacetate.

positional and isotropic thermal parameters are listed in Table IV.

Results and Discussion

Stereoscopic views of the β-maltose octaacetate molecules are shown in Figure 1. The numbering of the atoms, shown in Figure 2, proceeds from the nonreducing end (unprimed atoms) to the reducing end (primed atoms). The atoms in the acetate groups have been labeled CA, CM, and OA. These abbreviations stand for the carbonyl C, the methyl C, and the carbonyl O, respectively. O(61), CA(61), OA(61), CM(61) and O(62), CA(62), OA(62), CM(62) refer to the acetates with *tg* and *gt* orientations, respectively. The bond distances and angles in the molecule are given in Tables V and VI, respectively. All bond distances and angles conform to the tabulated values for oligosaccharides.[5] However, some of the C(61) acetate results are anomalous, especially the short O(61)–CA(61) distance, the long CA(61)–OA(61) distance, and the large C(6)–O(61)–CA(61) angle to which are associated high thermal parameters. Inhabitual bond distances and angles often observed in conjunction with atomic disorder have previously been encountered in acetylated oligosaccharides such as β-cellobiose octaacetate,[9] cellotriose undecaacetate,[10] methyl 6-*O*-acetyl-D-glucopyranoside,[23] and methyl 6-*O*-acetyl-β-galactopyranoside.[24] Such disorder of the C(6) acetate group must be considered a regular feature of acetylated crystalline oligosaccharides.

The Glycosidic Linkage. The relative orientation of contiguous pyranosides is customarily described by the torsion angles around the glycosidic bonds, C(1)–O(1) and O(1)–C(4′), and are denoted as the conformational angles Φ and Ψ. The values of these torsional angles are Φ = H(1)–C(1)–O(1)–C(4′) = −29° and Ψ = C(1)–O(1)–C(4′)–H(4′) = −36°. Another important parameter is the valence angle τ = C(1)–O(1)–C(4′) which is equal to 117.5°. The distance between the hydrogen atoms H(1) and H(4′) about the interglycosidic bridge is 2.35 Å. The torsional and bridge angles about the glycosidic bonds, as found in the already solved structures of disaccharides with α(1→4) linkage, are compared in Table VII where it can be seen that the variations in angle Φ (−29 to +3°) are slightly less than in angle Ψ (−36 to +11°). This is the same trend found by comparing the Φ and Ψ values for cellobiose octaacetate with those of cellobiose. A plot of the distribution of the Φ angles in all reported α-linked D-glucose residues (Figure 3) indicates that, despite the wide variety of linkage types, the variation of Φ is indeed restricted and a binodal distribution is clearly revealed. The left part of the histogram, centered at −45° and ranging from −60 to −35°, corresponds to structures that do not exhibit any intramolecular hydrogen bonding. Conversely, the other node, centered at Φ = −10° and ranging from −20 to 0°, is associated with oligosaccharides having a hydrogen bond between contiguous residues. This holds true

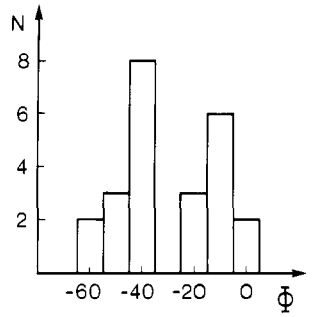

Figure 3. Distribution of the Φ torsion angle in α-linked oligosaccharides.

except for planteose[25] and corroborates a recent observation by Neuman.[26]

Ring Torsion Angles. The torsion angles about the various skeletal bonds of the pyranose rings are given in Table VIII. The expected $^4C_1$ conformation is found for both residues.[5] The ring conformation found in this structure is similar to that found in other peracetylated glucose residues, and the bond geometry conforms with the "standard glucose residue".[5,15] Significant effects on ring conformation due to acetylation are manifested in the exocyclic torsion angles such as O(2)–C(2)–C(1)–O(1) and O(2)–C(2)–C(3)–O(3).

Conformation of the C(6) Acetate Groups. The conformation of the primary acetate substituent at C(6) is described by the torsion angles O(5)–C(5)–C(6)–O(6) and C(5)–C(6)–O(6)–CA(6) referred to as χ(5), θ(6) and χ(5′), θ(6′) in the unprimed and primed residues, respectively. The conformation of the two primary acetate groups of the nonreducing residue is defined by χ(51) = 165°, θ(61) = −98° and χ(52) = 90°, θ(52) = 156°, whereas χ(5′) = −67° and θ(6′) = 148° are the values found for the primary acetate group at the reducing residue. Therefore, three different conformations are observed. According to the terminology proposed by Sundaralingam,[14] the conformation about χ(5′) is gauche–gauche (abbreviated *gg*), whereas the conformations of the C(6) acetate in the unprimed residue are *tg* and *gt*, respectively. The *tg* conformation is very unusual in oligosaccharides and has only been observed once previously[24] for methyl-6-*O*-acetyl-β-D galactopyranoside. As in the other carbohydrate acetates, the secondary acetate groups are arranged in such a way that the carbonyl O nearly eclipses the axial hydrogen atom at the corresponding ring carbon atoms.

Conformation Analysis. The potential energy was calculated by including the partitioned contributions arising from the nonbonded energies and torsion energies about the different torsion angles. The parameters used in this work are identical with those utilized previously in the study of potential energy of oligocellulose acetates.[15] The crystal structure coordinates were used and only the Φ and Ψ angles were allowed to vary. The energy map computed as a function of the rotations about the Φ and Ψ angles at intervals of 5° is given in Figure 4. With respect to the relative energy minimum, isoenergy contours were drawn by interpolation of energy. The 6 kcal mol^{-1} contour was selected as the outer limit. The observed crystallographic minimum (−29°, −36°) lies within the 1 kcal mol^{-1} region defined with respect to the calculated minimum (−65°, −45°). The 1 kcal mol^{-1} contour encompasses quite a wide domain, and the greater freedom of motion occurs for the Φ angle (from −70 to −15°). A second calculated minimum occurs at Φ = 35°, Ψ = 20°. This double-energy minimum inside the favored area is typical of the α(1→4) linked glucose residues. Upon extrapolation to amylose, this shows that both right- and left-handed helices are equally possible. Actually the presently found crystallographic minimum would generate a left-handed helix for the amylose acetate.

In the case of acetylated celluloses, the orientation of the primary acetate groups at C(6) has been shown to be an important

(23) K. B. Lindberg, *Acta Crystallogr., Sect. B*, **32**, 642 (1976).
(24) K. B. Lindberg, *Acta Crystallogr., Sect. B*, **32**, 645 (1976).
(25) D. C. Rohrer, *Acta Crystallogr., Sect. B*, **28** 425 (1972).
(26) A. Neuman, Thèse de doctorat, Université de Paris-Nord, France, 1980.

Table III. Anisotropic Thermal Parameters and Their Esd's in Parentheses ($\times 10^3$)[a]

ATOM	U11	U22	U33	U12	U13	U23
O(1)	57(2)	51(2)	66(2)	8(2)	-17(2)	7(2)
O(2)	56(3)	70(2)	62(2)	12(2)	2(2)	-18(2)
O(3)	54(2)	52(2)	86(3)	3(2)	2(3)	12(2)
O(4)	65(3)	98(3)	52(2)	3(3)	-5(2)	2(2)
O(5)	62(3)	66(2)	62(2)	-11(2)	-11(2)	-5(2)
O(61)	123(9)	112(8)	89(7)	-26(8)	-19(8)	-31(6)
O(62)	137(10)	81(6)	89(7)	-6(8)	16(8)	-1(5)
OA(2)	66(3)	154(5)	117(4)	7(4)	-14(3)	-68(4)
OA(3)	59(3)	85(3)	198(6)	2(3)	-10(4)	32(4)
OA(4)	133(5)	132(4)	80(3)	10(5)	14(4)	22(3)
OA(61)	171(13)	210(13)	85(7)	-22(13)	-18(9)	-57(8)
OA(62)	225(15)	118(8)	86(7)	22(11)	70(10)	-21(6)
C(1)	53(4)	59(3)	65(4)	5(3)	-12(3)	2(3)
C(2)	53(3)	50(3)	60(3)	4(3)	-1(3)	-5(3)
C(3)	50(3)	44(3)	60(3)	5(3)	-4(3)	1(3)
C(4)	55(4)	70(4)	53(3)	6(4)	-7(3)	-5(3)
C(5)	71(4)	64(4)	60(4)	-5(4)	-12(4)	-10(3)
C(6)	108(7)	117(6)	94(5)	-51(6)	-8(5)	-40(5)
CA(2)	78(5)	64(4)	71(4)	-3(4)	-3(4)	-19(3)
CA(3)	64(4)	63(4)	79(4)	-3(4)	3(4)	13(3)
CA(4)	91(6)	117(6)	60(4)	-19(5)	2(4)	1(4)
CA(61)	173(21)	95(11)	120(13)	16(15)	-28(16)	-25(11)
CA(62)	175(19)	85(10)	71(9)	-10(13)	35(12)	-20(8)
CM(2)	85(5)	76(4)	98(5)	-12(4)	1(5)	-25(4)
CM(3)	107(7)	66(5)	193(9)	-24(5)	30(8)	49(6)
CM(4)	132(9)	221(11)	61(4)	-51(9)	-26(6)	10(6)
CM(61)	211(30)	152(20)	136(18)	19(24)	3(22)	-18(16)
CM(62)	351(42)	136(18)	133(17)	44(28)	27(28)	-20(15)
O(1')	65(3)	56(2)	74(3)	6(2)	7(3)	3(2)
O(2')	77(3)	72(3)	55(2)	-6(3)	4(2)	-12(2)
O(3')	46(2)	57(2)	57(2)	0(2)	-3(2)	-15(2)
O(5')	61(3)	43(2)	63(2)	4(2)	-4(2)	-3(2)
O(6')	83(3)	99(3)	72(3)	20(3)	6(3)	-39(3)
OA(1')	60(3)	74(3)	120(4)	6(3)	2(3)	-13(3)
OA(2')	144(6)	206(7)	72(3)	-60(6)	-25(4)	3(4)
OA(3')	65(3)	76(3)	98(3)	-3(3)	4(3)	-38(3)
OA(6')	189(9)	221(8)	253(9)	-14(8)	-67(8)	-166(7)
C(1')	55(4)	50(3)	67(4)	-4(3)	3(3)	-1(3)
C(2')	52(3)	55(3)	53(3)	-7(3)	-2(3)	-8(3)
C(3')	51(3)	46(3)	58(3)	-1(3)	-7(3)	-12(3)
C(4')	54(4)	45(3)	58(3)	2(3)	-10(3)	-1(3)
C(5')	60(4)	49(3)	64(4)	5(3)	-15(3)	1(3)
C(6')	96(5)	72(4)	65(4)	27(4)	-30(4)	-1(3)
CA(1')	76(5)	55(4)	93(5)	6(4)	16(4)	-4(3)
CA(2')	121(7)	107(6)	60(4)	21(6)	5(5)	-10(4)
CA(3')	58(4)	63(4)	59(3)	10(3)	0(3)	-16(3)
CA(6')	120(8)	132(7)	113(6)	30(7)	0(7)	-65(6)
CM(1')	127(9)	103(6)	164(9)	29(7)	21(8)	30(6)
CM(2')	199(12)	180(9)	60(4)	25(11)	7(7)	-22(5)
CM(3')	76(5)	97(5)	84(5)	13(5)	-17(4)	-36(4)
CM(6')	110(8)	162(9)	211(11)	18(8)	57(9)	-100(9)

[a] The temperature factor is in the form: $T = \exp[-2\pi^2(U_{11}a^{*2}h^2 + \ldots + 2U_{12}a^*b^*hk + \ldots)]$.

factor in the establishment of the preferred conformations around Φ and Ψ.[12] In order to study the influence of the relative orientation of the primary acetate groups on the allowed conformations of maltose octaacetate, an energy map was computed on the deoxy analogue, i.e., with the primary acetate groups at C(6) and C(6′) removed. Only the 6 kcal mol^{-1} contour corresponding to this energy diagram is shown on Figure 4. It can be visualized that the obtained surface encompasses an area almost identical with the one defined by the 6 kcal mol^{-1} contour of maltose octaacetate. From this it can be concluded that in the case of peracetylated D-glucose residues linked α(1→4), the orientation of the substituent at C(6) and C(6′) does not have any major influence on the energetically allowed conformational space. This conclusion can be visualized from Figure 5. The α(1→4) linkage conformation places the acetate groups at C(6) and C(6′) on the same side of the molecule, and similarly for the secondary acetate groups at C(2) and C(3′). Therefore, the removal of the primary acetate groups does not suppress the nonbonded interactions occurring between the substituents at C(2) and C(3′); this explains the similarity between the two 6 kcal mol^{-1} energy contours, with and without the acetoxy groups. This is quite different from oligocellulose acetates where the β(1→4) linkage conformation induces a pseudo-2_1 helical conformation.[9,10] In the latter case, the primary acetate groups are located on opposite sides of the molecule, and they play an important role in establishing the preferred backbone conformation about Φ and Ψ.[11,12]

By superimposing on Figure 4 the 6 kcal mol^{-1} contour calculated for two α(1→4)-linked glucose residues,[27] one finds a near-topological and -positional identity of the contours for the nonacetylated and the peracetylated disaccharide. It follows that neither hydrogen bonding nor van der Waals forces emanating from substituents on primary and secondary hydroxylic oxygen atoms are crucial factors in establishing the overall features of the conformational domain of an α(1→4) glycosidic linkage.

Molecular Packing. The packing of the molecules in the unit cell is shown by the stereoscopic pair[28] in Figure 5. The molecules are held in the crystals by van der Waals forces only. The small

(27) S. Pérez, M. Roux, J. F. Revol, and R. H. Marchessault, *J. Mol. Biol.*, **129**, 113 (1979).

(28) M. L. Dheu and S Pérez, "PITMOS", Programmes Interactifs de Traces de Molécules et de Structures, CERMAV, Grenoble, France, 1980.

Table IV. Hydrogen Positional ($\times 10^3$) and Isotropic Thermal ($\times 10^3$) Parameters[a]

ATOM	X	Y	Z	U_{iso}
H(1)	-472	-681	-188	114
H(2)	-467	-774	-233	73
H(3)	-50	-738	-279	41
H(4)	-457	-752	-324	82
H(5)	-282	-646	-317	74
H(1')	282	-560	-112	64
H(2')	-213	-547	-92	65
H(3')	-49	-654	-121	74
H(4')	-327	-590	-188	54
H(5')	168	-597	-202	55
H(61')	114	-535	-267	60
H(62')	-7	-581	-273	112
HM(21)	79	-822	-134	63
HM(22)	-84	-872	-122	63
HM(23)	-86	-820	-85	63
HM(31)	71	-891	-358	82
HM(32)	-88	-918	-323	75
HM(33)	181	-916	-305	63
HM(41)	81	-769	-436	63
HM(42)	-21	-711	-459	63
HM(43)	-29	-768	-482	63
HM(11'	562	-415	-63	63
HM(12'	329	-428	-39	63
HM(13'	336	-389	-87	63
HM(21'	69	-613	40	63
HM(22'	-182	-620	61	63
HM(23'	-52	-564	69	63
HM(31'	-714	-682	-69	63
HM(32'	-611	-703	-17	63
HM(33'	-638	-744	-63	63
HM(61'	-583	-469	-264	63
HM(62'	-546	-451	-319	63
HM(63'	-453	-411	-279	63
H(611)	-690	-623	-335	63
H(612)	-713	-684	-355	63
H(621)	-751	-667	-336	63
H(622)	-576	-673	-382	63
HM(621	-684	-506	-382	63
HM(622	-640	-509	-442	63
HM(623	-893	-508	-420	63
HM(611	-347	-528	-399	63
HM(612	-500	-556	-357	63
HM(613	-252	-579	-368	63

[a] The isotropic thermal parameter is of the form: $T = \exp[-8\pi^2 U_{iso}(\sin^2\theta/\lambda^2)]$.

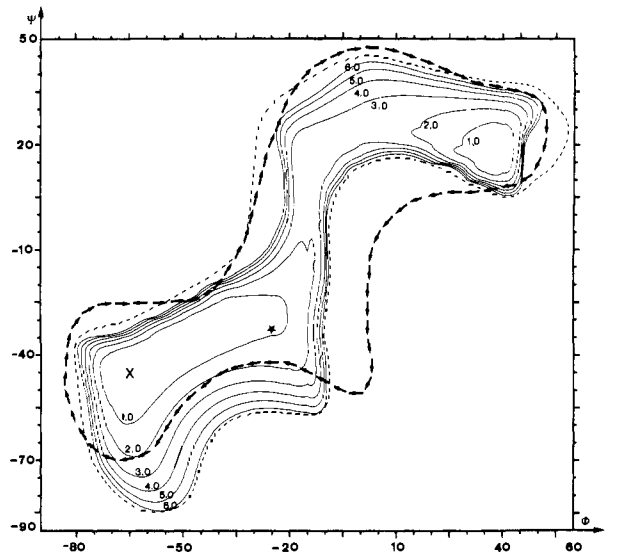

Figure 4. Energy diagram computed for β-maltose octaacetate. Contours were drawn by interpolation of energies computed at 5° in Φ and Ψ. The ☆ indicates the observed crystalline conformation, whereas × indicates the calculated absolute minimum. The 6 kcal mol^{-1} contours are shown as (- - -) and (→→→) for 6,6′-deoxy-β-maltose acetate and for β-maltose, respectively.

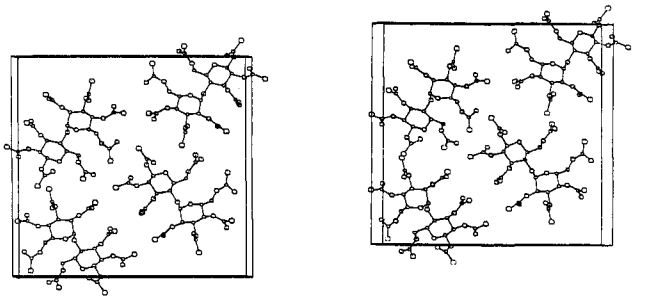

Figure 5. Packing of the molecules of β-maltose octaacetate (all molecules have the same conformation at C(6)).

value of the *a* parameter necessarily causes the molecules to lie parallel to the (100) plane.

Relation between β-Maltose Octaacetate and Amylose Triacetate. One of the stated purposes of this structure determination was to compare its main conformational features with those of the parent polysaccharide, amylose triacetate, whose structure was established some 15 years ago.

It is indeed very gratifying to observe (see Table IX) the high degree of similarity between the glycosidic torsion angles in β-maltose octaacetate and in amylose triacetate. Furthermore, the orientations of the acetate substituents are also very comparable. Had this structure been solved before the work on amylose triacetate was started, it would have provided the first experimental evidence for the *tg* conformation.

The indications obtained from this model compound as to some reasonable values for the glycosidic torsion angles and the acetate orientations would have been very useful in reducing the number

Table V. Bond Distances (and Their Esd's) in β-Maltose Octaacetate

C(1)-C(2)	1.519(7)	C(1)-O(1)	1.410(7)						
C(2)-C(3)	1.497(7)	C(2)-O(2)	1.446(7)	O(2)-CA(2)	1.328(7)	CA(2)-OA(2)	1.199(9)	CA(2)-CM(2)	1.491(10)
C(3)-C(4)	1.512(8)	C(3)-O(3)	1.438(6)	O(3)-CA(3)	1.337(8)	CA(3)-OA(3)	1.169(8)	CA(3)-CM(3)	1.474(9)
C(4)-C(5)	1.539(8)	C(4)-O(4)	1.435(7)	O(4)-CA(4)	1.344(8)	CA(4)-OA(4)	1.205(10)	CA(4)-CM(4)	1.462(11)
C(5)-C(6)	1.497(10)	C(5)-O(5)	1.426(7)						
		C(1)-O(5)	1.408(7)						
		C(6)-O(61)	1.355(12)	O(61)-CA(61)	1.156(19)	CA(61)-OA(61)	1.429(21)	CA(61)-CM(61)	1.279(27)
		C(6)-O(62)	1.268(12)	O(62)-CA(62)	1.392(18)	CA(62)-OA(62)	1.149(18)	CA(62)-CM(62)	1.458(24)
C(1')-C(2')	1.497(8)	C(1')-O(1')	1.419(6)	O(1')-CA(1')	1.371(8)	CA(1')-OA(1')	1.166(8)	CA(1')-CM(1')	1.501(11)
C(2')-C(3')	1.508(7)	C(2')-O(2')	1.437(6)	O(2')-CA(2')	1.360(9)	CA(2')-OA(2')	1.172(11)	CA(2')-CM(2')	1.484(11)
C(3')-C(4')	1.528(7)	C(3')-O(3')	1.446(7)	O(3')-CA(3')	1.377(6)	CA(3')-OA(3')	1.186(7)	CA(3')-CM(3')	1.482(9)
C(4')-C(5')	1.524(8)	C(4')-O(1)	1.438(6)						
C(5')-C(6')	1.510(8)	C(5')-O(5')	1.429(6)						
		C(6')-O(6')	1.390(9)	O(6')-CA(6')	1.332(9)	CA(6')-OA(6')	1.203(13)	CA(6')-CM(6')	1.450(14)
		C(1')-O(5')	1.407(7)						

Table VI. Bond Angles (and Their Esd's) in β-Octaacetate

C(1)-C(2)-C(3)	110.4(4)	O(1)-C(1)-O(5)	112.9(4)	O(4)-C(4)-C(3)	106.5(4)	O(2')-C(2')-C(1')	108.5(4)	C(5)-C(6)-O(61)	114.4(7)
C(2)-C(3)-C(4)	110.5(4)	O(1)-C(1)-C(2)	106.5(4)	O(4)-C(4)-C(5)	107.6(4)	O(2')-C(2')-C(3')	109.2(4)	C(6)-O(61)-CA(61)	135.1(13)
C(3)-C(4)-C(5)	111.7(5)			C(4)-O(4)-CA(4)	118.6(5)	C(2')-O(2')-CA(2')	116.9(5)	O(61)-CA(61)-OA(61)	123.4(17)
C(4)-C(5)-O(5)	111.1(5)	O(2)-C(2)-C(1)	111.3(4)	O(4)-CA(4)-OA(4)	122.8(7)	O(2')-CA(2')-OA(2')	124.3(7)	O(61)-CA(61)-CM(61)	108.7(18)
C(5)-O(5)-C(1)	114.8(4)	O(2)-C(2)-C(3)	105.6(4)	O(4)-CA(4)-CM(4)	111.0(6)	O(2')-CA(2')-CM(2')	108.1(7)	OA(61)-CA(61)-CM(61)	117.2(18)
O(5)-C(1)-C(2)	109.9(4)	C(2)-O(2)-CA(2)	119.1(4)	OA(4)-CA(4)-CM(4)	126.2(7)	OA(2')-CA(2')-CM(2')	127.6(8)		
		O(2)-CA(2)-OA(2)	121.7(6)					C(5)-C(6)-O(62)	123.9(8)
C(1)-O(1)-C(4')	117.5(4)	O(2)-CA(2)-CM(2)	111.2(5)	O(1)-C(4')-C(3')	110.5(4)	O(3')-C(3')-C(2')	108.9(4)	C(6)-O(62)-CA(62)	124.6(11)
		OA(2)-CA(2)-CM(2)	127.1(6)	O(1)-C(4')-C(5')	104.3(4)	O(3')-C(3')-C(4')	107.9(4)	O(62)-CA(62)-OA(62)	119.8(15)
C(1')-C(2')-C(3')	109.3(4)					C(3')-O(3')-CA(3')	117.3(4)	O(62)-CA(62)-CM(62)	112.9(16)
C(2')-C(3')-C(4')	111.7(4)	O(3)-C(3)-C(2)	109.3(4)	O(1')-C(1')-C(2')	107.5(4)	O(3')-CA(3')-OA(3')	122.9(5)	OA(62)-CA(62)-CM(62)	127.0(18)
C(3')-C(4')-C(5')	110.2(4)	O(3)-C(3)-C(4)	107.1(4)	O(1')-C(1')-O(5')	107.6(4)	O(3')-CA(3')-CM(3')	109.9(5)		
C(4')-C(5')-O(5')	110.3(4)	C(3)-O(3)-CA(3)	118.7(4)	C(1')-O(1')-CA(1')	114.5(4)	OA(3')-CA(3')-CM(3')	127.2(6)	C(5')-C(6')-O(6')	109.6(5)
C(5')-O(5')-C(1')	112.0(4)	O(3)-CA(3)-OA(3)	123.5(6)	O(1')-CA(1')-OA(1')	124.7(6)			C(6')-O(6')-CA(6')	119.5(6)
O(5')-C(1')-C(2')	109.6(4)	O(3)-CA(3)-CM(3)	109.6(6)	O(1')-CA(1')-CM(1')	110.0(6)	C(4)-C(5)-C(6)	110.4(5)	O(6')-CA(6')-OA(6')	119.1(8)
		OA(3)-CA(3)-CM(3)	126.9(6)	OA(1')-CA(1')-CM(1')	125.3(7)	O(5)-C(5)-C(6)	105.7(5)	O(6')-CA(6')-CM(6')	112.5(7)
						C(4')-C(5')-C(6')	113.5(5)	OA(6')-CA(6')-CM(6')	128.2(9)
						O(5')-C(5')-C(6')	106.6(5)		

Table VII. Torsion and Bridge Angles (deg) about the Glycosidic Bonds in Disaccharides with α(1→4) Linkage

	Φ H(1)-C(1)-O(1)-C(4')	Ψ C(1)-O(1)-C(4')-H(4')	τ C(1)-O(1)-C(4')	ref
β-maltose octaacetate	−29	−36	117.5	this work
α-maltose	−5	2	120.1	*a*
β-maltose	3	11	117.1	17, 18
β-methyl maltoside	−8	9	117.6	19
phenyl α-maltoside molecule A	−10	−20	116.5	*b*
molecule B	−10	−20	116.8	

[a] F. Takusawaga and R. A. Jacobson, *Acta Crystallogr., Sect. B*, **34**, 213 (1978). [b] I. Tanaka, N. Tanaka, T. Ashida, and M. Kakudo, *ibid.*, **32**, 155 (1976).

Table VIII. Torsion Angles (deg) with Estimated Errors of 2°

Torsion Angles about the Glycosidic Bond	unprimed residue	primed residue	oligocellulose acetate	standard β-D-glucose[5]
O(5)-C(1)-O(1)-C(4') = 84.0 C(1)-O(1)-C(4')-C(5') = −154.8				
Endocyclic Torsion Angles				
O(5)-C(1)-C(2)-C(3)	58.7	60.0	57.0	57.5
C(1)-C(2)-C(3)-C(4)	−54.7	−52.7	−54.2	−53.2
C(2)-C(3)-C(4)-C(5)	50.4	49.1	52.8	52.2
C(3)-C(4)-C(5)-O(5)	−49.4	−52.1	−58.0	−56.0
C(4)-C(5)-O(5)-C(1)	55.5	61.9	65.4	62.4
C(5)-O(5)-C(1)-C(2)	−60.0	−65.9	−64.8	−62.7
Exocyclic Torsion Angles[a]				
O(1)-C(1)-C(2)-O(2)	53.1	−64.3	−69.2	−63.6
O(2)-C(2)-C(3)-O(3)	67.3	69.8	71.2	64.6
O(3)-C(3)-C(4)-O(4)	−73.5	−76.6	−73.4	−67.0
O(4)-C(4)-C(5)-C(6)	77.1	69.8	65.8	63.7

[a] Note that O(4) in the primed residue is O(1).

of models examined in order to arrive at the structure of amylose triacetate.

Application to the Behavior of β-Maltose Octaacetate in Solution. The conformational behavior of a disaccharide in solution arises essentially from rotations about the glycosidic angles, which may be expressed by the distance between hydrogen atoms H(1) and H(4'). Such a distance can be evaluated using proton spin–lattice relaxation data (T_1) as obtained from nuclear magnetic resonance.

Since it has been established that the orientations of the primary acetate groups at C(6) and C(6') do not influence the overall shape of the (Φ, Ψ) map, it may be postulated that the so-defined domain contains all the possible conformations of the disaccharide in vacuo. Furthermore, it may be envisaged that the occurrence of a given conformation, within the defined domain, is energy independent. Such an assumption has indeed been successful in predicting the polysaccharide chain shapes in vacuo[29] and has been shown to yield results comparable to those arrived at by the simulation based on a Monte Carlo approach.[30]

Table IX. Comparison of β-Maltose Octaacetate and Amylose Triacetate

	β-maltose octaacetate	Amylose triacetate[2]
C(1)-O(1)-C(4')	117.5	113.3
C(1)-O(1)-C(4')-C(3')	87	70
C(1)-O(1)-C(4')-C(5')	-155	-171
C(4')-O(1)-C(1)-O(5)	84	81
C(4')-O(1)-C(1)-C(2)	-155	-158
Φ = H(1)-C(1)-O(1)-C(4')	-29	-39
Ψ = C(1)-O(1)-C(4')-H(4')	-36	-50
O(1)-C(1)-C(2)-O(2)	53 -64	57
O(2)-C(2)-C(3)-O(3)	67 70	70
O(3)-C(3)-C(4)-O(4)	-73 -77	-71
χ[O(5)]=O(5)-C(5)-C(6)-O(6)	166 91 -66	151
χ[C(4)]=C(4)-C(5)-C(6)-O(6)	-74 -149 55	-89
ω(6)=C(5)-C(6)-O(6)-CA(6)	-99 156 148	180

Table X. H(1)-H(4') Distance (Å) Determined from NMR Experiments Compared with the Simulated Result

T_1 measurements			
(I)[a] C_6D_6	(I)[a] $CDCl_3$	(II)[b] $CDCl_3$	simulation (III)[c]
2.23	2.46	2.42	2.48 (39)

[a] Trideuteriomethyl 2,3,6-tri-*O*-trideuterioacetyl-4-*O*-(2,3,4,6-tetra-*O*-trideuterioacetyl-α-D-glycopyranosyl)-β-D-glucopyranoside. [b] Methyl 2,3,6-tri-*O*-acetyl-4-*O*-(2,3,4,6-tetra-*O*-acetyl-α-D-glucopyranosyl)-β-D-glucopyranoside. [c] 1,2,3,6-tetra-*O*-acetyl-4-*O*-(2,3,4,6-tetra-*O*-acetyl-α-D-glucopyranosyl)-β-D-glucopyranoside.

The domain, defined by the 6 kcal mol^{-1} contour, was divided into a grid of 5° in Φ and Ψ and the H(1)–H(4') distance computed at each point. The distances so obtained range from 2.0 to 3.3 Å and average 2.48 Å (σ = 0.39). This value compares well with those obtained from T_1 experiments shown in Table X. The mean value is only slightly larger than the solution measurements. The difference may be attributed, in part, to the lack of interaction with solvent molecules in the simulation. Actually,

(29) D. Gagnaire, S. Pérez, and V. Trahn, *Carbohyd. Polym.*, **2**, 171 (1982).
(30) R. C. Jordan, D. A. Brant, and A. Cesar, *Biopolymers*, **17**, 2617 (1978).

it is clear that there is a solvent effect since values obtained in $CDCl_3$ differ slightly from those obtained in C_6D_6. Nevertheless, the overall agreement between simulated and observed values is quite satisfactory and would indicate that the proposed simulation does reflect the conformational flexibility of the molecule and can be a valid tool in investigating conformational behavior in solution.

Acknowledgment. The writers are grateful to Professor D. Horton for giving us the sample used in this analysis. We also wish to thank Dr. K. Bock for making the T_1 NMR data available prior to publication. This work was supported by the National Sciences and Engineering Research Council of Canada and the Ministère de l'Education du Québec.

Registry No. β-Maltose octaacetate, 22352-19-8; amylose triacetate, 9040-62-4.

Separability of Endovesicular and Exovesicular Reactions

Robert A. Moss,* Yasuji Ihara,[1a] and George O. Bizzigotti[1b]

Contribution from the Wright and Rieman Laboratories, Department of Chemistry, Rutgers, The State University of New Jersey, New Brunswick, New Jersey 08903. *Received May 19, 1982*

Abstract: *p*-Nitrophenyl diphenyl phosphate (**3**) was cleaved in vesicles of *N,N*-dihexadecyl-*N,N*-dimethylammonium bromide (**1**) or *N,N*-dihexadecyl-*N*-(β-hydroxyethyl)-*N*-methylammonium bromide (**2**) in 0.01–0.1 M aqueous NaOH at 25 °C. When the substrate was bound to and entrapped by the vesicle before addition of the base, initiation of the reaction gave consecutive "fast" and "slow" pseudo-first-order processes, assigned to exovesicular and endovesicular reactions, respectively. When the substrate was added to preformed vesicles, only the exovesicular cleavage could be observed. It was shown by experiments with vesicle-entrapped indigo carmine that permeation of hydroxide ions was not rate-limiting in endovesicular cleavage reactions.

The vigorous investigation of synthetic surfactant vesicles[2] as chemically unique reaction media continues apace.[3] Vesicles possess exterior and interior membrane surfaces and interior volumes which can entrap reagents and substrates.[2,4] These architectural elements constitute specific reaction sites, so that attention now focuses on the separability of *exovesicular* and *endovesicular* reactions. Three approaches may be identified. (a) "Unsymmetrical" vesicles can be produced by chemical differentiation of the exterior and interior vesicle surfaces.[5-7] (b) A "complex" surfactant may generate two distinct, "insulated" binding sites upon vesicle formation.[8] (c) Exovesicular and endovesicular reactions may be directly observed in *native* vesicles; e.g., kinetically distinct exterior and interior esterolyses of *p*-nitrophenyl acetate were observed with fully functionalized thiol vesicles.[9]

In this report, we generalize approach (c), demonstrating that simple, unfunctionalized, synthetic vesicles support the kinetic separability of exovesicular and endovesicular reactions.

Results and Discussion

Vesicles of dihexadecyldimethylammonium bromide (**1**, 16_2)

$$(n\text{-}C_{16}H_{33})_2N^+Me_2,Br^-$$
1 (16_2)

or dihexadecyl-β-hydroxyethylmethylammonium bromide (**2**, 16_2OH)[9] were generated from the surfactants by injection[9] or

$$(n\text{-}C_{16}H_{33})_2N^+MeCH_2CH_2OH,Br^-$$
2 (16_2OH)

sonication[2] in water. Substrate *p*-nitrophenyl diphenyl phosphate (**3**) was introduced by *coinjection* or *cosonication* with the surfactant at pH 7 (method A), or by *subsequent* addition *after* the vesicles had been formed (method B). Initiation of the cleavage of **3** was accomplished by stopped-flow combination of (vesicles + substrate) at pH 7 with aqueous NaOH (final concentrations 0.01–0.1 M) (method A), or by stopped flow combination of substrate in pH 7 water with vesicles in NaOH solutions (method B).[10] Reactions were followed by monitoring the appearance of *p*-nitrophenolate ion at 392 nm, and rate constants were evaluated from photographs of absorbance vs. time as displayed on an oscilloscope.

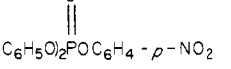

3

As shown in Table I, the kinetics of method A phosphate cleavage in vesicular **1** or **2** were biphasic or triphasic. They featured a "fast" pseudo-first-order process (k_ψ^f), accounting for 71–95% of reaction, followed by a "slow" (k_ψ^s) pseudo-first-order

(1) (a) Visiting Scholar from Yamaguchi Women's University, Yamaguchi, Japan. (b) Special Graduate School Fellow, Rutgers University.
(2) (a) Fendler, J. H. *Acc. Chem. Res.* **1980**, *13*, 7. (b) Kunitake, T.; Shinkai, S. *Adv. Phys. Org. Chem.* **1980**, *17*, 435. (c) Fendler, J. H. "Membrane Mimetic Chemistry"; Wiley: New York, in press.
(3) (a) Kunitake, T.; Okahata, Y.; Shimomura, M.; Yasunami, S-i; Takarabe, K. *J. Am. Chem. Soc.* **1981**, *103*, 5401. (b) Shimomura, M.; Kunitake, T. *Chem. Lett.* **1981**, 1001. (c) Murakami, Y.; Nakano, A.; Yoshimatsu, A.; Fukuya, K. *J. Am. Chem. Soc.* **1981**, *103*, 728. (d) Kunitake, T.; Okahata, Y.; Ando, R.; Shinkai, S.; Hirakawa, S-I. *Ibid.* **1980**, *102*, 7877. (e) Kunitake, T.; Nakashima, N.; Shimomura, M.; Okahata, Y.; Kano, K.; Ogawa, T. *Ibid.* **1980**, *102*, 6642. (f) Murakami, Y.; Nakano, A.; Fukuya, K. *Ibid.* **1980**, *102*, 4253.
(4) (a) Tran, C. D.; Klahn, P. L.; Romero, A.; Fendler, J. H. *J. Am. Chem. Soc.* **1978**, *100*, 1622. (b) Kunitake, T.; Sakamoto, T. *Ibid.* **1978**, *100*, 4615.
(5) Baumgartner, E.; Fuhrhop, J-H. *Angew. Chem., Int. Ed. Engl.* **1980**, *19*, 550.
(6) Tundo, P.; Kurihara, K.; Kippenberger, J.; Politi, M.; Fendler, J. H. *Angew. Chem., Int. Ed. Engl.* **1982**, *21*, 81.
(7) Fuhrhop, J.-H.; Bartsch, H.; Fritsch, D. *Angew. Chem., Int. Ed. Engl.* **1981**, *20*, 804.
(8) Murakami, Y.; Aoyama, Y.; Nakano, A.; Tada, T.; Fukuya, K. *J. Am. Chem. Soc.* **1981**, *103*, 3951.
(9) Moss, R. A.; Bizzigotti, G. O. *J. Am. Chem. Soc.* **1981**, *103*, 6512.
(10) It is shown below that OH^- permeation of the vesicles under method A is rapidly driven by substantial (5–6 units) pH gradients, and is not rate-limiting in the observed cleavages of **3**.

0002-7863/82/1504-7476$01.25/0